Effect of bed roughness on the propagation of negative surges in rivers and estuaries

X. LENG[a], H. CHANSON[a]

a. *The University of Queensland, School of Civil Engineering, Brisbane Q4072, Australia*

Résumé:

Dans un canal à surface libre où la hauteur d'eau aval décroit avec le temps, on observe une onde négative. Ce type d'écoulements correspond aussi à la marée descendante dans les estuaires avec des marnages importants, ainsi que le rundown (retraite) d'un tsunami après avoir atteint une côte maximale. Dans cette contribution, on discute l'effet de la rugosité de fond sur la propagation des ondes négatives, en se basant sur une analyse fine de mesures physiques, complémentée par une étude théorique. Les mesures en laboratoire ont été conduites dans un canal de 12 m de long et 0,5 m de large, et trois types de rugosité ont été testées systématiquement. Les résultats sont discutés dans le contexte de la littérature scientifique, avec des implications pratiques pour la gestion des estuaires et la protection des zones côtières sujettes à des tsunamis.

Abstract:

In an open channel, a sudden drop in water elevation is associated with a negative surge. Practical applications include the ebb tide motion in estuaries with macro-tidal conditions, the rundown of the swash, and the retreat of tsunami waters after reaching the maximum runup. Herein a physical study is presented with a focus on the effects of bed roughness. Detailed measurements were performed in a large facility with three roughness types. The results are presented and practical applications are discussed.

Mots clefs : Ondes négatives, Rugosité de fond, Ecoulements à surface libre, Ecoulement instationnaire

Keywords : Negative surges, Bed roughness, Open channel flow, Unsteady flow

1 Introduction

In a canal, a sudden increase in water depth is called a positive surge or bore which is a flow discontinuity characterised by a steep front. A sudden decrease in water depth, called a negative surge, is characterised by a gentle change in free-surface elevation (Fig. 1). It may occur upstream of an opening gate, as well as downstream of a closing gate (Henderson 1966, Liggett 1994, Reichstetter and Chanson 2013). Some geophysical applications include the ebb tide flow in macro-tidal estuaries, the rundown of swash waters and the retreating waters after maximum tsunami runup. During the 26 December 2004 and 11 March 2011 tsunami disasters, visual and video observations showed a large amount of damage, including sediment scour, caused by the negative surges and associated turbulent mixing.

In this contribution, a physical study is presented with a focus on the effects of bed roughness on negative surge propagation. Detailed measurements were performed in a large facility with three roughness types. Free-surface measurements were conducted and the results were ensemble-averaged. Additional unsteady velocity measurements were conducted to highlight the unsteady turbulent mixing.

2 Physical modelling and instrumentation

The physical study of negative surges is typically performed with a geometrically similar model. For the simple case of a negative surge propagating in a rectangular horizontal prismatic canal after a sudden and

complete gate opening, a dimensional analysis gives a series of relationship between the unsteady flow properties at a point in space (x, y, z) and time t as functions of the initial flow conditions, canal geometry and fluid properties:

$$\frac{d}{d_o}, \frac{P}{\rho g d_o}, \frac{V_x}{V_o}, \frac{V_y}{V_o}, \frac{V_z}{V_o}, \frac{v_x'}{V_o}, \frac{v_y'}{V_o}, \frac{v_z'}{V_o} = F\left(\frac{x}{d_o}, \frac{y}{d_o}, \frac{z}{d_o}, t\sqrt{\frac{g}{d_o}}, \frac{V_o}{\sqrt{g d_o}}, \frac{v_o'}{\sqrt{g d_o}}, \rho \frac{V_o d_o}{\mu}, \frac{g \mu^4}{\rho \sigma^3}, \frac{B}{d_o}, \frac{k_s}{d_o}, ... \right) \quad (1)$$

where d is the water depth, P the pressure, V is the velocity component, v is a turbulent velocity fluctuation, the subscript x, y and z correspond to the longitudinal, transverse and vertical velocity components, d_o and V_o are respectively the initial flow depth and velocity (Fig. 1), g is the gravity acceleration, ρ and μ are the fluid density and viscosity, σ is the surface tension, B is the channel width and k_s is a roughness height. In open channel flows, the gravity effects are important and a Froude similitude is commonly used (Henderson 1966, Liggett 1994). This is also the case in the present study. In Equation (1), note the absence of the initial gate opening h and flow rate Q which are implicitly accounted for in the initial flow conditions (d_o, V_o).

New experiments were performed in a 12 m long 0.5 m wide horizontal channel, made of smooth PVC bed and 0.30 m high glass walls (Table 1). The experimental flow conditions are summarised in Table 1. The waters were supplied by a constant head tank. A fast opening tainter gate was located at the downstream end (x = 11.12 m) where x is the distance from the channel upstream end. The water discharge was measured with an orifice meter calibrated on site. In steady flows, the water depths were measured with rail mounted pointer gauges. The unsteady water depths were recorded with Microsonic™ Mic+25/IU/TC acoustic displacement meters spaced along the channel at x = 11.25, 10.9, 10.6, 10.3, 8, 6.5, 5 and 3.5 m. The velocity measurements were conducted at x = 5 m with an acoustic Doppler velocimeter (ADV) Nortek™ Vectrino+ equipped with a side-looking head. For the experiments, the velocity range was 1.0 m/s. All the instruments were sampled at 200 Hz and all measurements were conducted on the centreline. Additional informations were recorded with a Pentax™ K-7 dSLR camera and Sony™ HDR-SR11E HD video camera.

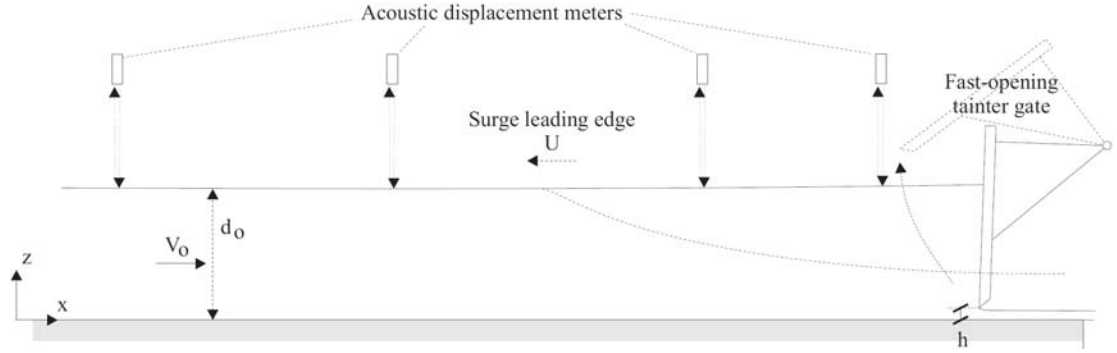

FIG. 1 – Definition sketch of a negative surge propagating upstream against an initially steady flow

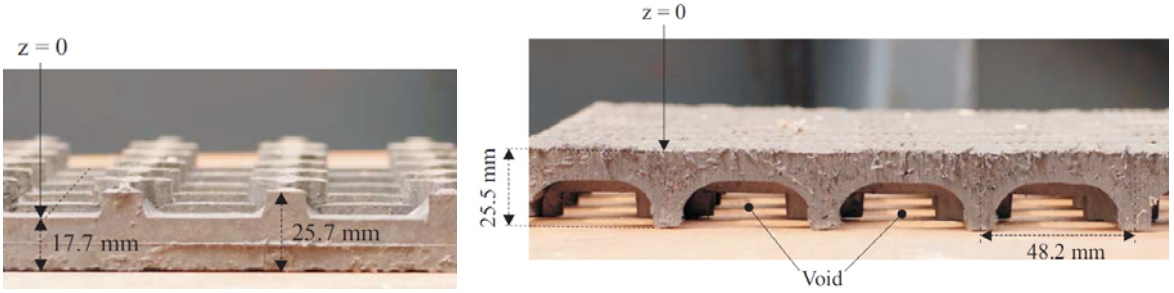

FIG. 2 – Rubber mat configurations A (upward spikes, left) and B (downward spikes, right)

Three types of bed roughness were tested systematically. Some experiments were performed with the smooth PVC bed. For the other experiments, the PVC invert was covered with a series of industrial rubber floor mats for 0.075 < x < 11.10 m. The rubber mats consisted of square patterns cut to the channel width: configuration A and B (Fig. 2). The configuration B corresponded to the conventional floor mat setting, allowing some continuous gaps between the PVC and rubber floor (Fig. 2, right). The hydraulic conductivity of the material was tested, yielding a hydraulic conductivity K ≈ 0.14 m/s and permeability k ≈ 1.4×10^{-8} m^2. The hydraulic roughness of the PVC invert and rubber mat configurations was tested for a range of steady flow

conditions. The bed shear stress was deduced from the measured free-surface profiles and friction slopes. The Darcy friction factor of the PVC bed ranged from 0.020 to 0.050 corresponding to mean equivalent sand roughness height k_s = 1 mm. The equivalent Darcy friction factor of the rubber mat sheets was f_{matA} = 0.09 to 0.18 and f_{matB} = 0.05 to 0.09 for configurations A and B respectively, corresponding to k_s = 39 mm (Config. A) and 12 mm (Config. B) on average. Such rugosity heights were comparable to the rubber mat thickness (Fig. 2).

The experimental flow conditions are summarised in Table1 , together with the tests of Reichstetter and Chanson (2013). The key features herein were the detailed measurements for larger discharges and Reynolds numbers, combined with systematic experiments of three bed roughness configuration.

Table 1 - Experimental investigations of negative surges

Reference	Q (m^3/s)	Bed roughness	h (m)	d_o (m)	U (m/s)	$\rho \frac{V_o d_o}{\mu}$	Instrumentation
Reichstetter and Chanson (2013)	0.020 & 0.030	PVC	0.030 to 0.050	0.10 to 0.26	0.25 to 0.91 ([1])	4.0×10^4 & 6.0×10^4	Video imagery
	0.020	PVC	0.030	0.24	0.91 ([1])	4.0×10^4	Acoustic displacement meters & ADV Vectrino+.
Present study	0.025	PVC	0.045 to 0.070	0.107 to 0.23	0.5 to 1.25 ([2])	5.0×10^4	Acoustic displacement meters.
	0.035	PVC	0.075 to 0.090	0.128 to 0.181	0.53 to 0.94	6.8×10^4	
	0.025	Rubber mat config. A	0.060 to 0.073	0.156 to 0.222	1.01 to 1.41	5.0×10^4	Acoustic displacement meters & ADV Vectrino+.
	0.035	Rubber mat config. A	0.085 to 0.092	0.180 to 0.210	0.83 to 1.11	6.8×10^4	
	0.025	Rubber mat config. B	0.060 to 0.070	0.15 to 0.23	0.81 to 1.09	5.0×10^4	Acoustic displacement meters.
	0.035	Rubber mat config. B	0.080 to 0.082	0.18 to 0.197	0.95 to 1.04	6.8×10^4	

Notes: Q: initial steady flow rate; S_o=0: horizontal bed slope; d_o, V_o: initial flow depth and velocity recorded at sampling location; U: celerity of negative surge leading edge positive upstream measured at ([1]) x = 6 m or ([2]) x = 5 m.

3 Basic observations

Visual, photographic and video observations showed a steep drop of the water surface next to the gate immediately after the gate opening (Fig. 3 & 4). Figures 3 and 4 show some series of photographs of gate opening with nearly identical initial flow conditions on smooth and rough beds respectively. In Figures 3 & 4, Q is the initially steady flow rate, d_o is the initial flow depth at x = 5 m and h is the undershoot gate opening (before rapid opening). In both Figures 3 and 4, the initially steady discharge flowed from left to right, and the negative surge propagated from right to left. The observations highlighted the rapid gate opening (less than 0.2 s) and negative wave formation, although the free-surface profile exhibited a smooth surface very rapidly, within one second. The instantaneous free-surface exhibited a very-smooth shape further upstream: the free-surface was very flat and the visual observations indicated the gradual lowering of the water surface during the upstream propagation of the negative surge. The upstream propagation of the negative wave leading edge was barely perceptible, but next to the gate immediately after opening.

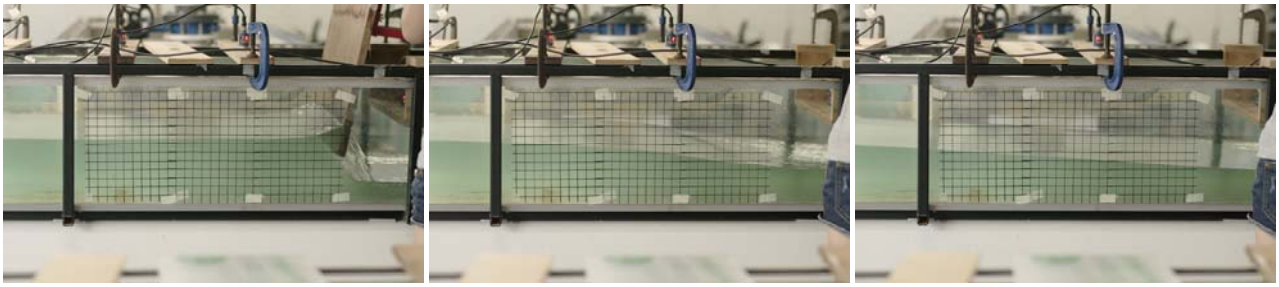

FIG. 3 – Negative surge generation above smooth PVC invert - Q = 0.0254 m^3/s, d_o = 0.155 m, h = 0.055 m, t = t_o, t_o + 0.77 s, t_o + 1.35 s (Left to right)

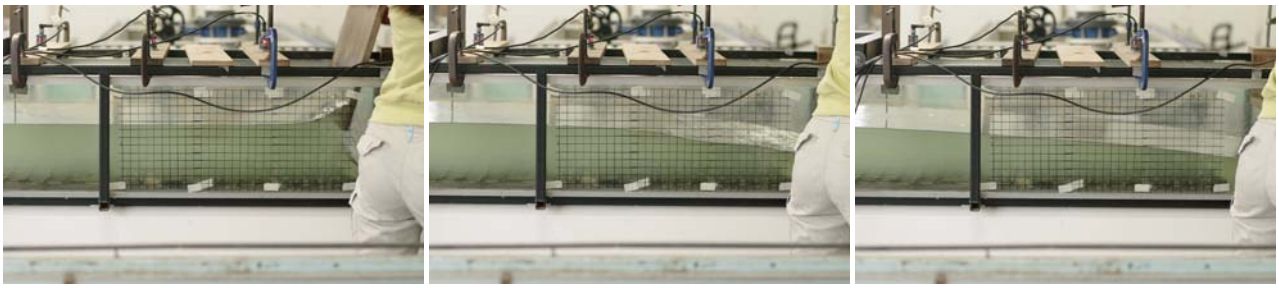

FIG. 4 – Negative surge generation above rough bed (rubber mat configuration A) - Q = 0.0254 m^3/s, d_o = 0.156 m, h = 0.073 m, t = t_o, t_o + 0.77 s, t_o + 1.35 s (Left to right)

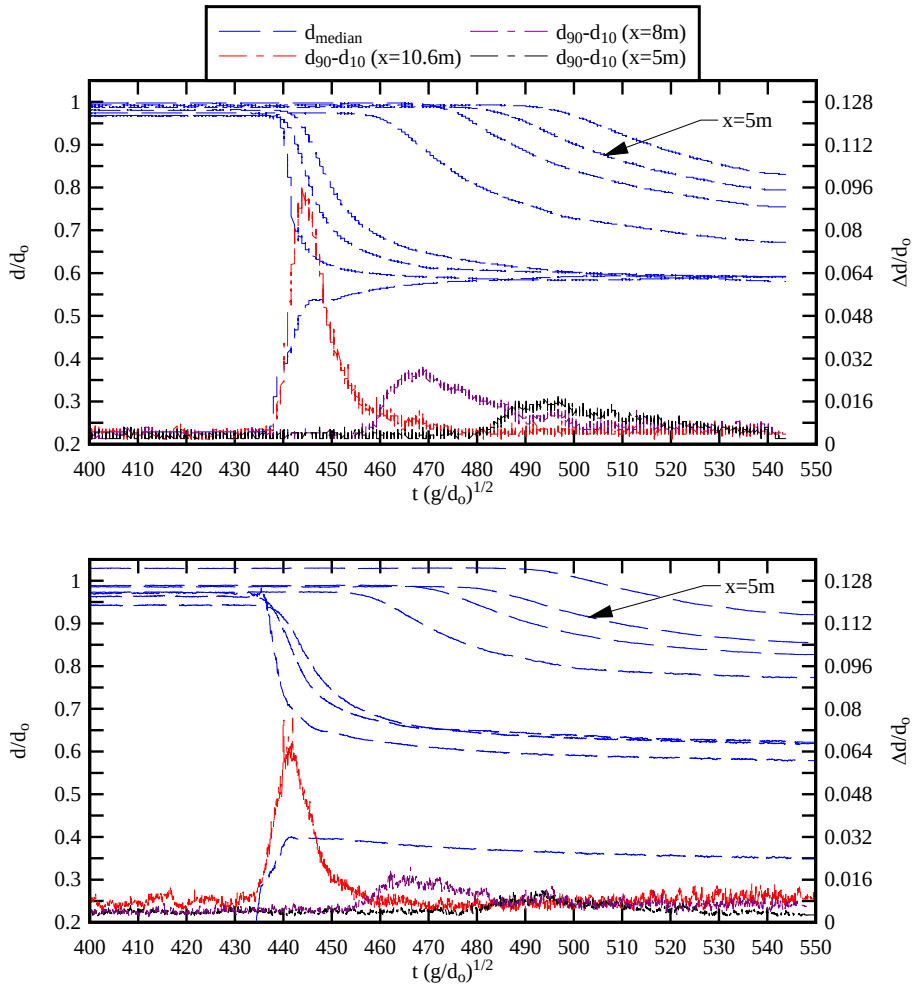

FIG. 5 – Ensemble-averaged time variations of water depth and differences between 90% and 10% percentiles (d_{90}-d_{10}) in negative surges - Average over 25 runs, water depths at x = 11.25, 10.9, 10.6, 10.3, 8.0, 6.5, 5.0 and 3.5 m - (A, Top) Q = 0.0345 m^3/s, d_o = 0.1825 m, h = 0.075 m, smooth PVC invert; (B, Bottom) Q = 0.0345 m^3/s, d_o = 0.1803 m, h = 0.092 m, rubber mat configuration A

During the negative surge, the water depth decreased relatively gradually after the rapid generation phase. The free surface measurements showed some surface curvature near the surge leading edge (Fig. 5). Figure 5 presents some ensemble-averaged free-surface measurements at several longitudinal locations. Both the ensemble-median, and the difference between the ninth and first deciles (d_{90}-d_{10}) are presented. All the free-surface data highlighted the gentle free-surface profile at the surge leading edge. The free-surface curvature and slope were larger close to the gate than further upstream, but the radius of curvature was quantitatively large, implying quasi-hydrostatic pressure distributions. For all experiments, the data showed large fluctuations in free-surface elevations associated with the propagation of the surge leading edge. The maximum free-surface fluctuations decreased exponentially with increasing distance from the gate as

illustrated in Figures 5A and 5B.

The celerity of the negative wave leading edge was recorded using a combination of photographic, video and acoustic displacement meter data. Figure 6 presents a typical data set, where L is the test section length (L = 12 m). The gate location is indicated with thick vertical line. Both ensemble-averaged results and single run data are included. The data showed the same distinct trend for all bed configurations. Immediately after the gate opening, the negative wave formed very rapidly (Fig. 3 & 4). The celerity of its leading edge increased rapidly with time, reaching maximum dimensionless value in excess of 2: that is, $(U+V_o)/(g\times d_o)^{1/2} > 2$. This acceleration phase was associated by some strong flow disturbance next to the gate. Further upstream, the negative wave leading edge propagated in a more gradual manner during which its leading celerity decreased exponentially with time towards $(U+V_o)/(g\times d_o)^{1/2} = 1$ where V_o is the initial flow velocity at x = 5 m (Fig. 6). For all the bed configurations, the surge celerity tended to an asymptotic value ($(U+V_o)/(g\times d_o)^{1/2} = 1$) which is the analytical solution of the St Venant equations (Henderson 1966, Chanson 2004). Quantitatively, the bed roughness had little effect on the surge celerity, although the unsteady free-surface profiles appeared visually flatter in presence of large bed roughness.

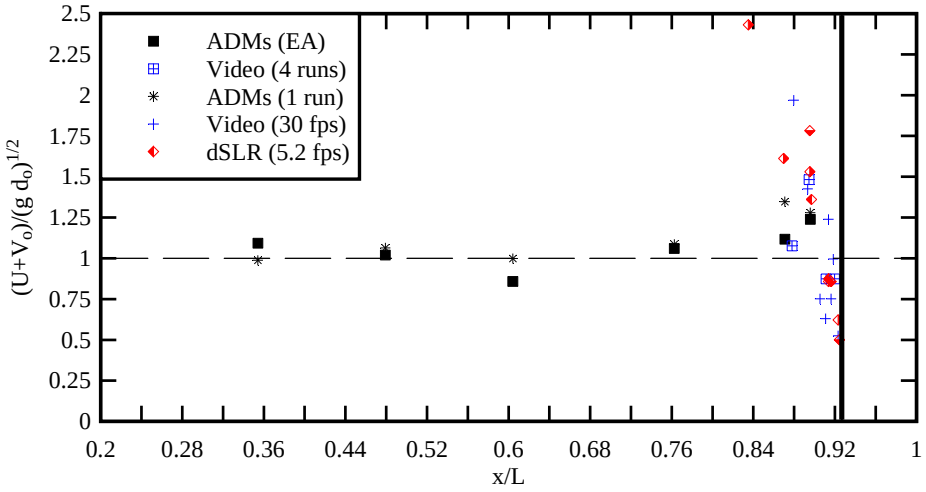

FIG. 6 – Celerity of negative surge leading edge along the test section - Comparison between acoustic displacement meter (ADM) data (ensemble-average and 1 run), video observations (ensemble average and 1 run) and dSLR data - Q = 0.0254 m^3/s, d_o = 0.155 m, h = 0.055 m, smooth PVC invert

4 Unsteady velocity measurements

Detailed unsteady velocity measurements were conducted for two flow rates on the roughest bed configuration (rubber mat config. A) (Table 1). Typical results are shown in Figure 7. The longitudinal velocity increased at the same time as the water depth decreased. That is, the data showed some flow acceleration during the rundown of the water surface which was linked with some increase in all velocity component fluctuations, compared to the initially steady flow conditions. For example, for $t\times(g/d_o)^{1/2} = 360$ to 410 and 410 to 440 in Figures 7A and 7B respectively. Figures 7A and 7B present some dimensionless time-variations of instantaneous velocity components for the same run at two vertical elevations: i.e., z/d_o= 0.24 and 0.69 at x = 5 m, together with the free-surface elevations at several longitudinal locations. A comparative analysis showed the effect of the vertical elevation: namely, the acceleration was more significant in the upper water column (z/d_o = 0.69, Fig. 7). The present findings were consistent with and extended the findings of Reichstetter and Chanson (2013). All in all, the data showed that the negative wave flow was a highly unsteady turbulent process.

5 Conclusion

The properties of negative surges propagating against an initially steady flow were investigated in laboratory in a large size facility. Both non-intrusive free-surface measurements and intrusive velocity measurements were conducted for relatively large Reynolds numbers with three types of bed roughness, thus expanding the initial findings of Reichstetter and Chanson (2013) on smooth bed..

The dimensionless results showed little effect of the bed roughness, within the experimental flow conditions.

The propagation of the negative surge appeared to be gentle rundown, but both the free-surface fluctuations and turbulent velocity fluctuations were large beneath the leading edge of the negative surge. Such conditions are favourable to bed scour and sediment entrainment during the surface rundown. The surge celerity data showed some characteristic trend, with a rapid acceleration, the deceleration of the leading edge, before the surge celerity satisfied: $(U+V_o)/(g\times d_o)^{1/2} = 1$.

In practical applications, such as the ebb tide flow in a macro-tidal estuary and the retreat of tsunami waters after maximum runup, bed erosion will occur as the surge leading edge propagates upstream, thus placing the sediment material into suspension before it is re-entrained downstream in the accelerated rundown flow.

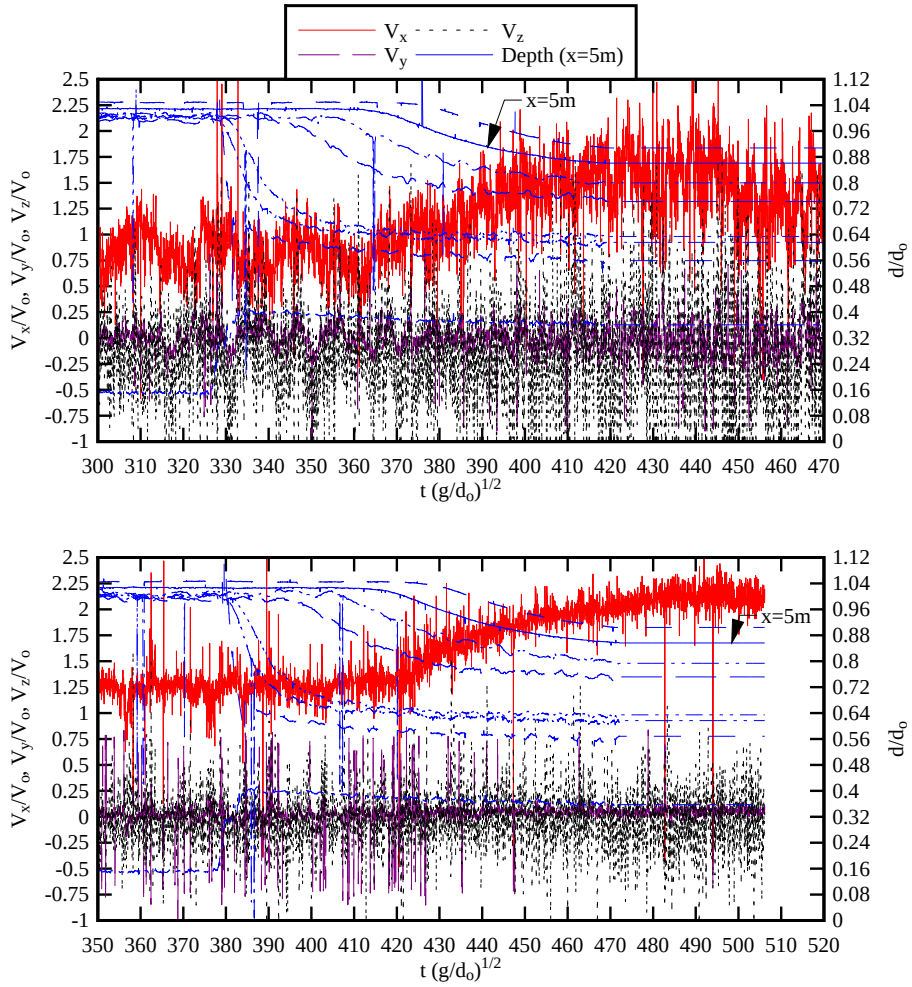

FIG. 7 – Instantaneous Eulerian velocity measurements beneath a negative surge - Q = 0.0345 m^3/s, d_o = 0.2013 m, V_o = 0.343 m/s, h = 0.085 m, z/d_o = 0.24 (A, Top) & 0.69 (B, Bottom), rubber mat configuration A - Single run, water depths at x = 11.25, 10.9, 10.6, 10.3, 8.0, 6.5, 5.0 and 3.5 m, velocity data at x = 5 m

6 Acknowledgements

The writers acknowledge the financial support of the Australian Research Council (Grant DP120100481) and the technical assistance of Jason Van Der Gevel and Matthews Stewart (University of Queensland).

References

Chanson, H. (2004). The Hydraulics of Open Channel Flow: An Introduction. Butterworth-Heinemann, 2nd edition, Oxford, UK, 630 pages.
Henderson, F.M. (1966). Open Channel Flow. MacMillan Company, New York, USA.
Liggett, J.A. (1994). Fluid Mechanics. McGraw-Hill, New York, USA.
Reichstetter, M., and Chanson, H. (2013). Unsteady Turbulent Properties in Negative Waves in Open Channels. *European Journal of Mechanics B/Fluids*, Vol. 37, pp. 1-9 & 2 movies (DOI: 10.1016/j.euromechflu.2012.07.003).